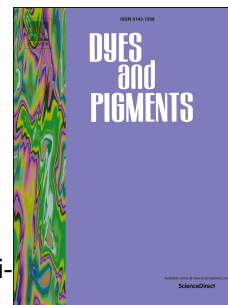


Journal Pre-proof

Chiral thermally activated delayed fluorescence emitters with dual conformations based on a pair of enantiomeric donors containing asymmetric carbons

Feng-Yan Hao, Yi-Zhong Shi, Kai Wang, Shi-Yun Xiong, Xiao-Chun Fan, Lin Wu, Cai-Jun Zheng, Yan-Qing Li, Xue-Mei Ou, Xiao-Hong Zhang



PII: S0143-7208(20)30377-6

DOI: <https://doi.org/10.1016/j.dyepig.2020.108336>

Reference: DYPI 108336

To appear in: *Dyes and Pigments*

Received Date: 11 February 2020

Revised Date: 6 March 2020

Accepted Date: 6 March 2020

Please cite this article as: Hao F-Y, Shi Y-Z, Wang K, Xiong S-Y, Fan X-C, Wu L, Zheng C-J, Li Y-Q, Ou X-M, Zhang X-H, Chiral thermally activated delayed fluorescence emitters with dual conformations based on a pair of enantiomeric donors containing asymmetric carbons, *Dyes and Pigments* (2020), doi: <https://doi.org/10.1016/j.dyepig.2020.108336>.

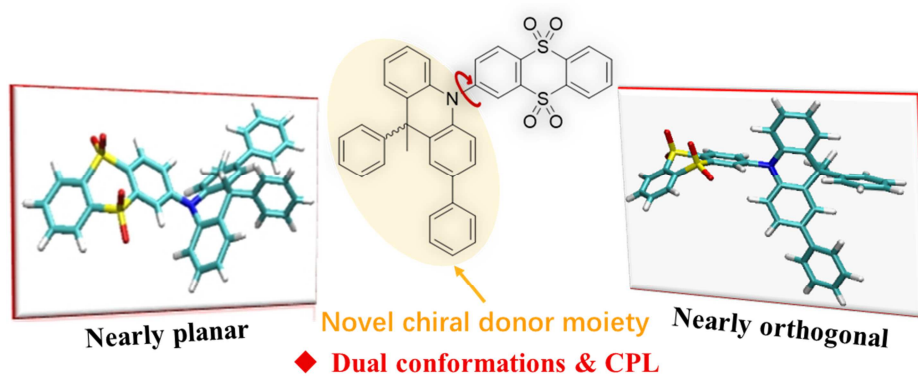
This is a PDF file of an article that has undergone enhancements after acceptance, such as the addition of a cover page and metadata, and formatting for readability, but it is not yet the definitive version of record. This version will undergo additional copyediting, typesetting and review before it is published in its final form, but we are providing this version to give early visibility of the article. Please note that, during the production process, errors may be discovered which could affect the content, and all legal disclaimers that apply to the journal pertain.

© 2020 Published by Elsevier Ltd.

Hao Feng-Yan: Investigation, Formal analysis, Visualization **Shi Yi-Zhong:** Project administration, Writing - Original Draft **Wang Kai:** Conceptualization, Methodology, Writing - Original Draft **Xiong Shi-Yun:** Writing - Original Draft **Fan Xiao-Chun:** Investigation **Wu Lin:** Validation **Zheng Cai-Jun:** Methodology **Li Yan-Qing:** Methodology **Ou Xue-Mei:** Methodology **Zhang Xiao-Hong:** Resources, Supervision

Journal Pre-proof

Graphical Abstract



Journal Pre-proof

Chiral thermally activated delayed fluorescence emitters with dual conformations based on a pair of enantiomeric donors containing asymmetric carbons

Feng-Yan Hao,^a Yi-Zhong Shi,^a Kai Wang,^{*a} Shi-Yun Xiong,^a Xiao-Chun Fan,^a Lin Wu,^a Cai-Jun Zheng,^{*b} Yan-Qing Li,^a Xue-Mei Ou^a and Xiao-Hong Zhang^{*a}

^aInstitute of Functional Nano & Soft Materials (FUNSOM), Jiangsu Key Laboratory for Carbon-Based Functional Materials & Devices, Soochow University, Suzhou, Jiangsu 215123 (P.R. China)

^bSchool of Optoelectronic Science and Engineering, University of Electronic Science and Technology of China (UESTC), Chengdu, Sichuan 610054 (P.R. China)

E-mail addresses: wkai@suda.edu.cn (K.W.), zhengcaijun@uestc.edu.cn (C.-J.Z.), xiaohong_zhang@suda.edu.cn (X.-H.Z.).

Keywords: Chirality, Thermally activated delayed fluorescence, Dual stable conformations, Circular dichroism, Circularly polarized luminescence

Abstract

Thermally activated delayed fluorescence (TADF) chiral emitters attract widespread attention due to their high exciton utilization as well as potential applications. In this work, we developed a pair of chiral donors, (*R*) and (*S*)-9-methyl-2,9-diphenyl-9,10-dihydroacridine (PMAc), for general TADF molecular design. The enantiomers (*R*) and (*S*)-TTR-PMAc are accordingly constructed. Interestingly, they are not only TADF emitters, but also possess dual stable conformations, i.e. nearly planar and nearly orthogonal conformations. (*R*) and (*S*)-TTR-PMAc show similar physical properties under conventional non-polarized environment. While under chiroptical environments, they exhibit obvious mirror-like

circular dichroism (CD) and circularly polarized luminescence (CPL) properties. Moreover, by further comparing the CPL properties originated from each conformer, we confirm that molecular conformations can significantly influence the chiroptical performance.

1. Introduction

Circularly polarized luminescence (CPL) attracts widespread attentions because of its potential applications in 3D imaging, information storage and quantum computing [1-3]. Generally, it can be obtained by employing polarizer and quarter-wave plate from the non-polarized light. However, these methods not only induce serious energy loss, but also complicate device architectures [4, 5]. In contrast, developing novel chiral organic dyes is more attractive as they can generate CPL directly.

Recently, thermally activated delayed fluorescence (TADF) emitters are of the hotspot in the whole organic optoelectronic field, as they can utilize not only singlet excitons, but also triplet excitons via efficient reversed intersystem crossing (RISC) process [6-11]. Correspondingly, developing TADF emitters with CPL properties is highly desired. Currently, several CPL-TADF emitters have been reported by introducing additional chiral moieties, such as 1,1'-bi-2-naphthol, 1,2-diaminocyclohexane and [2.2]paracyclophane, into TADF frameworks [12-17]. In these compounds, chiral moieties are additional burdens for TADF properties. Their introduction needs dedicated molecular designs and extra synthetic procedures. Thus, it is difficult to extend these strategies to the design of other TADF emitters.

TADF emitters are generally constructed by combining electron-donor (D) and electron-acceptor (A) segments with highly twisted morphology to fulfil

the requirement of small singlet-triplet energy splitting (ΔE_{ST}) [18-26]. It is highly desired to directly develop chiral D and A segments and use them to construct chiral TADF emitters. In this work, we developed a pair of novel chiral D enantiomers with asymmetric carbon atoms, (*R*)- and (*S*)-9-methyl-2,9-diphenyl-9,10-dihydroacridine (PMAc), which can be easily applied to general TADF molecular design. We further combine them with a strong A segment thianthrene 5,5,10,10-tetraoxide (TTR) to construct a pair of enantiomers ((*R*) and (*S*)-TTR-PMAc). Interestingly, they are not only TADF emitters, but also possess dual stable conformations, i.e. nearly planar and nearly orthogonal conformations [27-31]. Like other CPL-TADF emitters [12, 13, 15, 16, 32-36], owing to the opposite chiral active core, the circular dichroism (CD) spectra of (*R*)- and (*S*)-TTR-PMAc in dilute toluene solution depict an obvious mirror-image relationship. On the other hand, the molecules with nearly planar and nearly orthogonal conformations exhibit different specific circular properties, which eventually induces the enantiomers to display opposite circularly polarized luminescence (CPL) properties. These results not only prove that (*R*)- and (*S*)-PMAc are ideal candidates for constructing CPL-TADF emitters, but also demonstrate that the chiroptical properties can be significantly influenced by molecular conformations.

2. Experimental section

2.1. General

All reactants and solvents were purchased from commercial sources and used without further purification. Chiral supercritical fluid chromatography (SFC) was utilized to separate the enantiomers for analysis via the Waters ACQUITY UPCC with

the mobile phase of CO₂ and isopropanol (70: 30), the PDA as ultraviolet detector. ¹H NMR and ¹³C NMR spectra were recorded on a Bruker 400 and 600 spectrometer at room temperature. Mass spectra were recorded on a Nermag R10-10C spectrometer. The single-crystal X-ray diffraction data of single crystals were collected from a Bruker D8 Venture X-ray single crystal diffractometer. The CCDC reference number of chiral donor moiety (*R*)-PMAc (CCDC: 1975853) and the data can be obtained free of charge from The Cambridge Crystallographic Data Centre via www.ccdc.cam.ac.uk/data_request/cif. Chiral resolution and analyze of the chiral purity were carried out via a Waters ACQUITY UPCC. Circular dichroism (CD) and circularly polarized luminescence (CPL) spectra were measured on Jasco J-810 spectropolarimeter and Jasco CPL 300, respectively.

UV-vis absorption spectra were recorded on a Hitachi U-3900 spectrophotometer. PL spectra and phosphorescent spectra were recorded on a Hitachi F-4600 fluorescence spectrophotometer. Transient fluorescence decays were measured with a Quantaaurus-Tau fluorescence lifetime spectrometer (C11367-32, Hamamatsu Photonics) with the excitation wavelength of 373 nm and pulse width of 100 ps. Differential scanning calorimetry (DSC) was performed on a TA DSC 2010 unit at a heating rate of 10 °C·min⁻¹ under nitrogen environment. Thermogravimetric analysis (TGA) was performed on a TA SDT 2960 instrument at a heating rate of 10 °C·min⁻¹ with nitrogen protection. The temperature corresponds to 5% weight loss was used as the decomposition temperature (*T_d*).

Cyclic voltammetry (CV) was carried out on a CHI660E voltammetric analyzer at room temperature. Deaerated DMF was used as solvent with tetrabutylammonium hexafluorophosphate (TBAPF₆) (0.1 M) as the supporting electrolyte. The cyclic

voltammograms (CV) were obtained at the scanning rate of $0.05 \text{ V}\cdot\text{s}^{-1}$ with a gold electrode and a platinum wire as the working and counter electrodes and an Ag/AgCl electrode (3.0 M) as the reference electrode with standardized against ferrocene/ferrocenium.

Density functional theory (DFT) and time-dependent DFT (TD-DFT) calculations were performed at the B3LYP/6-31g (d) level of theory using Gaussian 09 program package [37, 38] and analyzed using a multifunctional wavefunction analyzer (Multiwfn 3.7) [39]. Potential energy surface (PES) scan of the ground state (*R*)- and (*S*)-TTR-PMac was stimulated under the polarizable continuum model (PCM) in tetrahydrofuran (THF).

2.2 Synthesis

2.2.1 Synthesis of 1-(2-([1,1'-biphenyl]-4-ylamino)phenyl)ethan-1-one (**a**)

A mixture of 4-bromo-1,1'-biphenyl (5.0 g, 21.0 mmol), 1-(2-aminophenyl)ethan-1-one (3.2 g, 23.6 mmol), Pd(OAc)₂ (0.24 g, 1.1 mmol), tri-tert-butylphosphine (2.0 mL, 3.2 mmol) and Cs₂CO₃ (14 g, 42.9 mmol) was stirred and refluxed in toluene (80 mL) overnight under the N₂. After cooled to room temperature and the solvent had been removed, the solid was purified by column chromatography on silica gel using petroleum ether/ dichloromethane (4/1, v/v) as the eluent to give **a** (3.6g) as a yellow solid; yield 58 %. ¹H NMR (600 MHz, DMSO-*d*₆) δ 10.47 (s, 1H), 7.98 (dd, *J* = 8.1, 1.7 Hz, 1H), 7.67 (t, *J* = 7.1 Hz, 4H), 7.45 (q, *J* = 7.2 Hz, 3H), 7.34 (dd, *J* = 8.6, 6.7 Hz, 4H), 6.86 (t, *J* = 7.6 Hz, 1H), 2.64 (s, 3H). ESI-MS (*m/z*): calcd. for C₂₀H₁₇NO 287.1310, found 287.1318.

2.2.2 Synthesis of 9-methyl-2,9-diphenyl-9,10-dihydroacridine (**PMac**)

1-(2-([1,1'-biphenyl]-4-ylamino)phenyl)ethan-1-one (3.5 g, 12.2 mmol) was

dissolved in tetrahydrofuran (60 mL) under argon and cooled to $-10\text{ }^{\circ}\text{C}$. Then phenylmagnesium bromide (1 M in THF, 25 mL, 25.0 mmol) was added dropwise under stirred. After 2 h reaction at $0\text{ }^{\circ}\text{C}$, the mixture was gradually warmed up to $35\text{ }^{\circ}\text{C}$ and stirred overnight. Then the reaction was quenched by water (2 mL). After cooled to room temperature, the solvent had been removed and the crude product was not further purified. The crude product was put into acetic acid (60 mL) and concentrated HCl (2 mL) mixed solution under air and was heated at $80\text{ }^{\circ}\text{C}$ for 5 h. When reaction was cooled to room temperature, ice water (80 mL) was poured into and then solid was filtered. The solids were purified by column chromatography on silica gel using petroleum ether/ dichloromethane (4/1, v/v) as the eluent to give **PMAc** (3.0 g) as a white solid; yield 69 %. ^1H NMR (600 MHz, $\text{DMSO-}d_6$) δ 9.15 (s, 1H), 7.40 – 7.32 (m, 5H), 7.29 (d, $J = 4.3\text{ Hz}$, 4H), 7.21 (t, $J = 7.2\text{ Hz}$, 1H), 7.17 (p, $J = 4.1\text{ Hz}$, 1H), 7.07 – 7.03 (m, 1H), 7.00 (d, $J = 2.0\text{ Hz}$, 1H), 6.92 (d, $J = 8.2\text{ Hz}$, 1H), 6.84 (d, $J = 7.9\text{ Hz}$, 1H), 6.76 (d, $J = 7.7\text{ Hz}$, 1H), 6.69 (t, $J = 7.4\text{ Hz}$, 1H), 1.88 (s, 3H). ESI-MS (m/z): calcd. for $\text{C}_{26}\text{H}_{21}\text{N}$ 347.1674, found 347.1680.

2.2.3 Synthesis of (*R*)- and (*S*)-2-(9-methyl-2,9-diphenylacridin-10(9*H*)-yl)thianthrene 5,5,10,10-tetraoxide ((*R*)- and (*S*)-**TTR-PMAc**)

A mixture of (*R*)-**PMAc** (0.52 g, 1.5 mmol) 2-bromothianthrene 5,5,10,10-tetraoxide (0.55 g, 1.5 mmol), $\text{Pd}(\text{OAc})_2$ (17 mg, 0.075 mmol), tri-*tert*-butylphosphine (0.1 mL, 0.23 mmol) and NaOt-Bu (0.36 g, 3.7 mmol) was stirred and refluxed in toluene (30 mL) for overnight under the N_2 . After cooled to room temperature and the solvent had been removed, the solids were purified by column chromatography on silica gel using petroleum ether/dichloromethane (4/1, v/v) as the eluent to give (*R*)-**TTR-PMAc** (0.66 g) as a white solid; yield 70 %. ^1H NMR

(400 MHz, DMSO- d_6) δ 8.37 – 8.28 (m, 3H), 8.10 – 8.02 (m, 2H), 7.96 (d, $J = 2.3$ Hz, 1H), 7.83 (dd, $J = 8.5, 2.3$ Hz, 1H), 7.58 – 7.52 (m, 2H), 7.50 – 7.38 (m, 4H), 7.35 – 7.29 (m, 1H), 7.28 – 7.16 (m, 2H), 7.14 – 7.02 (m, 5H), 6.90 – 6.76 (m, 3H), 2.07 (s, 3H). ^{13}C NMR (101 MHz, CDCl_3) δ 148.68, 147.87, 141.01, 140.49, 140.16, 140.08, 139.63, 139.46, 138.51, 138.03, 137.33, 133.66, 133.40, 132.90, 128.85, 128.10, 127.98, 127.68, 127.66, 127.27, 127.08, 126.95, 126.33, 126.28, 125.96, 125.71, 125.65, 124.40, 120.46, 120.12, 119.14, 46.65, 28.17. ESI-MS (m/z): calcd. for $\text{C}_{38}\text{H}_{27}\text{NO}_4\text{S}_2$ 625.7570, found 625.7575.

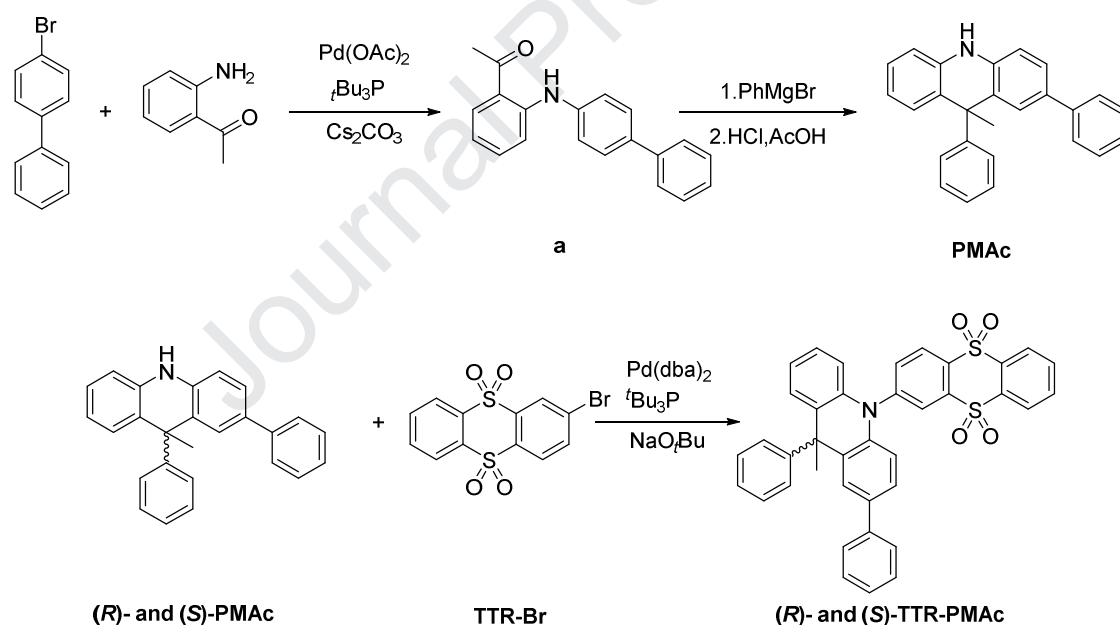
(*S*)-**TTR-PMAc** was prepared with a similar procedure of (*R*)-**TTR-PMAc** with (*S*)-PMAc instead of (*R*)-PMAc. (*S*)-**TTR-PMAc** (0.66 g) was obtained as a white solid; yield 70 %. ^1H NMR (400 MHz, DMSO- d_6) δ 8.36 – 8.26 (m, 3H), 8.09 – 8.01 (m, 2H), 7.95 (d, $J = 2.2$ Hz, 1H), 7.82 (dd, $J = 8.5, 2.3$ Hz, 1H), 7.56 – 7.50 (m, 2H), 7.48 – 7.38 (m, 4H), 7.31 (s, 1H), 7.26 – 7.15 (m, 2H), 7.13 – 7.02 (m, 5H), 6.89 – 6.75 (m, 3H), 2.05 (s, 3H). ^{13}C NMR (101 MHz, CDCl_3) δ 148.68, 147.87, 141.00, 140.49, 140.16, 140.08, 139.62, 139.45, 138.51, 138.03, 137.32, 133.66, 133.40, 132.90, 128.85, 128.10, 127.98, 127.68, 127.65, 127.27, 127.08, 126.95, 126.33, 126.28, 125.96, 125.71, 125.65, 124.40, 120.46, 120.13, 119.13, 46.65, 28.17. ESI-MS (m/z): calcd. for $\text{C}_{38}\text{H}_{27}\text{NO}_4\text{S}_2$ 625.7570, found 625.7575.

3. Results and discussion

3.1 Synthesis and characterization

Detailed experimental procedures of chiral segment (*R*)- and (*S*)-PMAc and the corresponding chiral TADF emitters (*R*)- and (*S*)-**TTR-PMAc** are demonstrated in Scheme 1. Racemic mixture precursor of PMAc are firstly synthesized according to the reported experimental procedure [40]. Followed with separation process via the

chiral supercritical fluid chromatography (SFC), novel enantiomers (*R*)- and (*S*)-PMAc were successfully obtained, which is further verified by the result of X-ray spectrum. (Fig. S1) Finally (*R*)- and (*S*)-TTR-PMAc are synthesized via Buchwald–Hartwig cross-coupling reaction between enantiomers (*R*)- and (*S*)-PMAc and the brominated derivative of the acceptor TTR. The chemical structures of intermediate compounds as well as final chiral emitters are well confirmed via the nuclear magnetic resonance (NMR), mass spectroscopy and analytical chiral SFC. As exhibited in Fig. S8, no obvious racemization is observed. The obtained enantiomers (*R*) and (*S*)-TTR-PMAc well maintained their purity before and after vacuum evaporation process, which proves the chiral stability induced by asymmetric carbon atoms.



Scheme 1. Experimental procedure of enantiomers (*R*)- and (*S*)-TTR-PMAc.

3.2 Theoretical simulations

To get deep insights on effect of the chiral segments, theoretical simulations are

investigated by density functional theory (DFT) at the level of B3LYP/6-31G*. Polarizable continuum model (PCM) in tetrahydrofuran (THF) is applied to predict the potential energy surface (PES) of (*R*)- and (*S*)-TTR-PMac in their ground states. As demonstrated in Fig. 1, both enantiomers depict nearly identical energy curves with dual stable valleys. The nearly planar conformations are the favourable conformation due to the lower energy, while the nearly orthogonal ones with TADF characteristics is the semi-stable state [28]. Optimal dihedral angles between the TTR and (*R*)- and (*S*)-PMac moieties are estimated to be 173.46° and 85.57°, corresponding to the nearly planar and orthogonal conformations, respectively. We further estimated the relative distributions of both conformers according to Boltzmann distribution. As listed in Table S2, both enantiomers are estimated to have similar conformational distributions. The relative ratios of the nearly planar and orthogonal conformations are estimated to be 97.6 and 2.4 % for (*R*)-TTR-PMac and 97.3 and 2.7 % for (*S*)-TTR-PMac, respectively. As shown in Fig. S4, both the nearly orthogonal molecules display negligible exchange integral from the highest occupied molecular orbital (HOMO) and lowest unoccupied molecular orbital (LUMO) distributions, benefiting the up-conversion of excitons from the lowest triplet (T_1) to singlet excited states (S_1). While large overlaps observed in their nearly planar conformations, indicating they are non-TADF conformers. Moreover, we further investigated their excited states by using the time-dependent density-functional-theory (TD-DFT) based on the optimal geometry in ground states. Fig. S4 illustrates their natural transition orbitals (NTOs) in S_1 and T_1 states with stable conformations. (*R*)- and (*S*)-TTR-PMac show similar distributions as well, and thus result in their similar oscillator strengths and ΔE_{ST} values. These results further indicate that the

introduction of chirality doesn't influence their energy levels and they may exhibit indistinguishable properties under non-polarized environment.

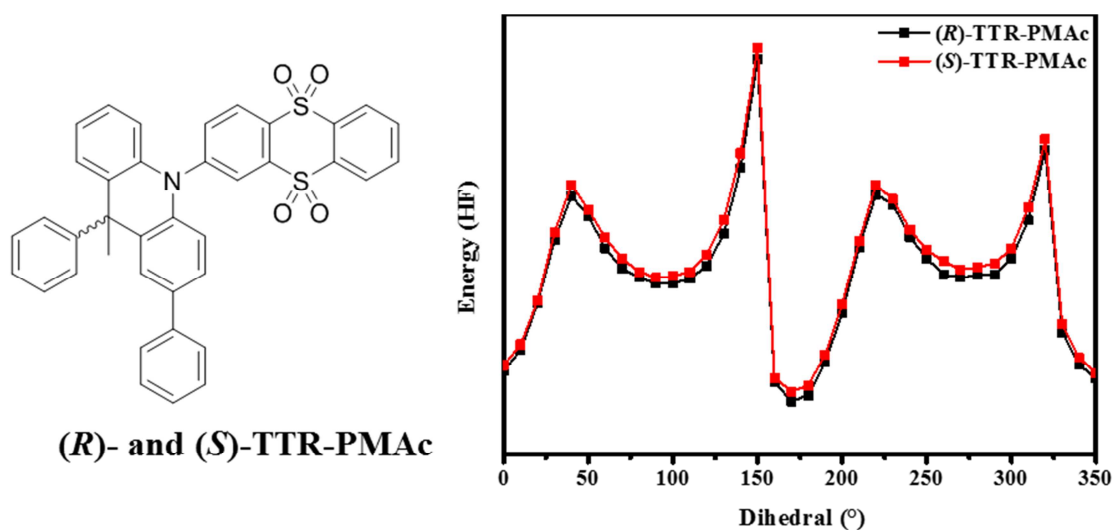


Fig.1 Molecular structure and potential energy surface (PES) scan of the ground state (*R*)- and (*S*)-TTR-PMaC under the polarizable continuum model (PCM) in tetrahydrofuran (THF).

3.3 Electrochemical and thermal properties

To confirm their identical energy levels, electrochemical properties of the enantiomers (*R*)- and (*S*)-TTR-PMaC are first studied by the cyclic voltammetry (CV) measurement. As summarized in Table 1, the enantiomers (*R*)- and (*S*)-TTR-PMaC depict nearly identical CV curves with HOMO/LUMO estimated to -5.66/-3.31 eV for (*R*)-TTR-PMaC and -5.69/-3.30 eV for (*S*)-TTR-PMaC, respectively, indicating chirality does not differentiate their HOMO and LUMO energy levels. Thermal stability of the target enantiomers as well as the racemic mixtures has also been measured via the thermogravimetric analysis (TGA) and differential scanning calorimetry (DSC). As shown in Fig. S3, they exhibit similar high decomposition temperature of 403~409 °C. On the other hand, both (*R*)- and (*S*)-TTR-PMaC

exhibit undetectable glass transition temperature (T_g), which is different from the racemic mixtures ($T_g = 148$ °C). These results further suggest the effective chiral retentions of (*R*)- and (*S*)-TTR-PMac and D modifications do not bring different side effects on their thermal stabilities.

3.4 Photophysical properties

Owing to the asymmetric molecular frameworks, the enantiomers (*R*)- and (*S*)-TTR-PMac display indistinguishable photophysical properties under non-polarized measurements. As illustrated in Fig. 2a, in dilute toluene, they both exhibit two typical intramolecular charge-transfer (ICT) absorption bands. The strong adsorption bands centred at 357 nm are associated with the nearly planar conformations; while the weak one at 400 nm can be ascribed to the highly twisted nearly orthogonal conformations. Correspondingly, from their emission spectra in toluene at room temperature, there are two broad and structureless emission bands with the observed peak wavelength at ~430 and 577 nm. Moreover, by diluting them in different solvents with varied polarities, a synchronous redshift solvatochromic effect can be observed for both enantiomers (Fig. S5). The emission from nearly planar molecules depict a relatively small redshift of ~30 nm with increasing solvent polarity from hexane to dichloromethane; while the nearly orthogonal conformations display more significant bathochromic shift, suggesting their ICT characteristics.

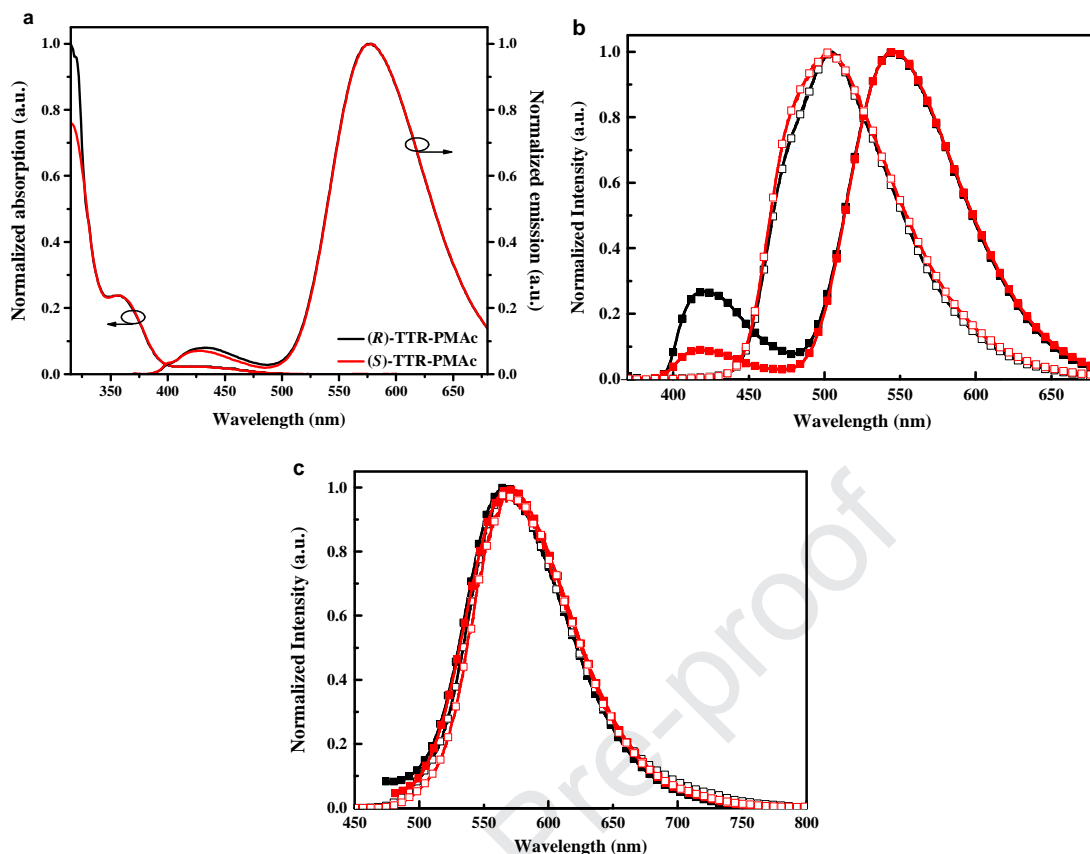


Fig.2 a) The UV/Vis absorption spectra and fluorescent spectra of (*R*)- (black) and b) (*S*)-TTR-PMAc (red) in dilute toluene solution (10⁻⁵ M); Normalized fluorescence (solid), phosphorescence (hollow) spectra b) in 2-MeTHF and c) the pristine films at 77 K.

To further compare their energy levels for both conformations, fluorescence and phosphorescence spectra of both chiral emitters are measured in different conditions at 77 K. In dilute 2-methyltetrahydrofuran (2-MeTHF), S_1 and T_1 levels of nearly planar molecules can be clearly figured out, and the ΔE_{ST} is estimated to be as large as 0.36 and 0.39 eV for (*R*)-TTR-PMAc and (*S*)-TTR-PMAc, respectively. Therefore, triplet excitons can hardly be utilized in these conformations. While in neat films, only spectra from nearly orthogonal conformations can be observed, resulting in much smaller ΔE_{ST} of 0.02 and 0.05 eV, indicating they possess TADF properties. Transient PL decays of target chiral emitters are further measured to confirm their TADF

characteristics. Fig. S6 shows their fluorescence spectra and corresponding transient fluorescence decay curves in diluted toluene. Comparing, under an air atmosphere, the orange emission originated from nearly orthogonal conformations depict a significant enhancement after degassing with nitrogen, while the minor deep blue emission does virtually not change, suggesting their opposite exciton utilizations in different conformations. Likewise, from the transient decay curves, two exponential decays can be observed clearly from the emission from the nearly orthogonal conformations with high oxygen sensitivity; while at deep blue region, the lifetimes change only slightly. These results prove that the modification of chirality does not change the TADF properties of dual conformations.

Table 1 Summary of key physical properties of chiral TADF emitters.

Molecules	$\lambda_{\text{PL}}^{\text{a}}$ (nm)	$\Delta E_{\text{ST}}^{\text{b}}$ (eV)	$\tau_{\text{p}}^{\text{d}}$ (ns)	$\tau_{\text{d}}^{\text{d}}$ (μs)	HOMO/LUMO ^e (eV)	T_{d}^{f} ($^{\circ}\text{C}$)
(<i>R</i>)-TTR-PMAC	436/577	0.36 ^b /0.02 ^c	27.0	0.43	-5.66/-3.31	405
(<i>S</i>)-TTR-PMAC	427/577	0.39 ^b /0.05 ^c	26.8	0.47	-5.69/-3.30	403

Determined from ^aUV-vis absorption spectra and fluorescent spectra measured in dilute toluene solution. Determined from the onset of the fluorescence/phosphorescence spectrum in ^b2-MeTHF and ^cthe neat film measured in 77K, ΔE_{ST} calculated as $\Delta E_{\text{ST}} = S_1 - T_1$. ^dLifetime of chiral emitters, the prompt and delayed component in transient PL in dilute toluene solution. ^eHOMO was determined from the onset of oxidation potential with respect to ferrocene; LUMO was determined from the onset of reduction potential with respect to ferrocene. ^fdecomposition temperature, corresponding to 5% weight loss.

3.5 Chiral photophysical properties

Although under conventional non-polarized environment, the enantiomers show nearly identical properties, their differences are obvious under chiroptical environment. Fig. S7 illustrates the circular dichroism (CD) spectra of chiral D segments (*R*)- and (*S*)-PMAC and of the resulted D-A enantiomers in toluene. (*R*)- and (*S*)-PMAC shows obvious mirror-like spectra in their absorptions ranges below 350 nm. Correspondingly, the mirror-like properties are well maintained

for the D-A enantiomers. In particular for the local excited area shorter than 340 nm, strong CD intensities can be obtained, which is inherited from the D segments. Moreover, in the ICT absorption range of 350~450 nm, weak mirror-like images can be also obtained. These results suggest that the chiral PMAc has successfully induced chirality in the enantiomers in their ground states.

More importantly, the opposite chirality of the enantiomers in different configurations are expected to induce different CPL properties. To clarify it, we first measured their spin-coated pristine films, where the nearly orthogonal conformers dominate the emission spectra. As shown in Fig. 3b, clearly mirror-like CPL can be found in the range of 500~700 nm, consistent with the emission range of nearly orthogonal molecules, suggesting they are CPL-active conformers. On the other hand, to explore the CPL properties of nearly planar conformations, the powder samples of both enantiomers are prepared by sublimation process and scattered between two transparent quartz plates. As shown in Fig. 3c, the nearly orthogonal molecules clearly dominate the emission spectra with strong deep blue emission peaked at 425 nm for both enantiomers; while the yellow emissions only show weak shoulders. Likewise, from their CPL spectra (Fig. 3d), almost mirror-image can be observed at the whole emission range. Thus, we can clearly notice that the chiral segments endow not only nearly orthogonal conformers, but also nearly planar ones and with chiroptical properties in their S_1 states. Interestingly, in each enantiomer, their CPL signals from nearly planar and nearly orthogonal conformations shows opposite dissymmetry factors. This result indicates that molecular conformations with different electronic structures and transition properties can significantly influence chiroptical properties

[41].

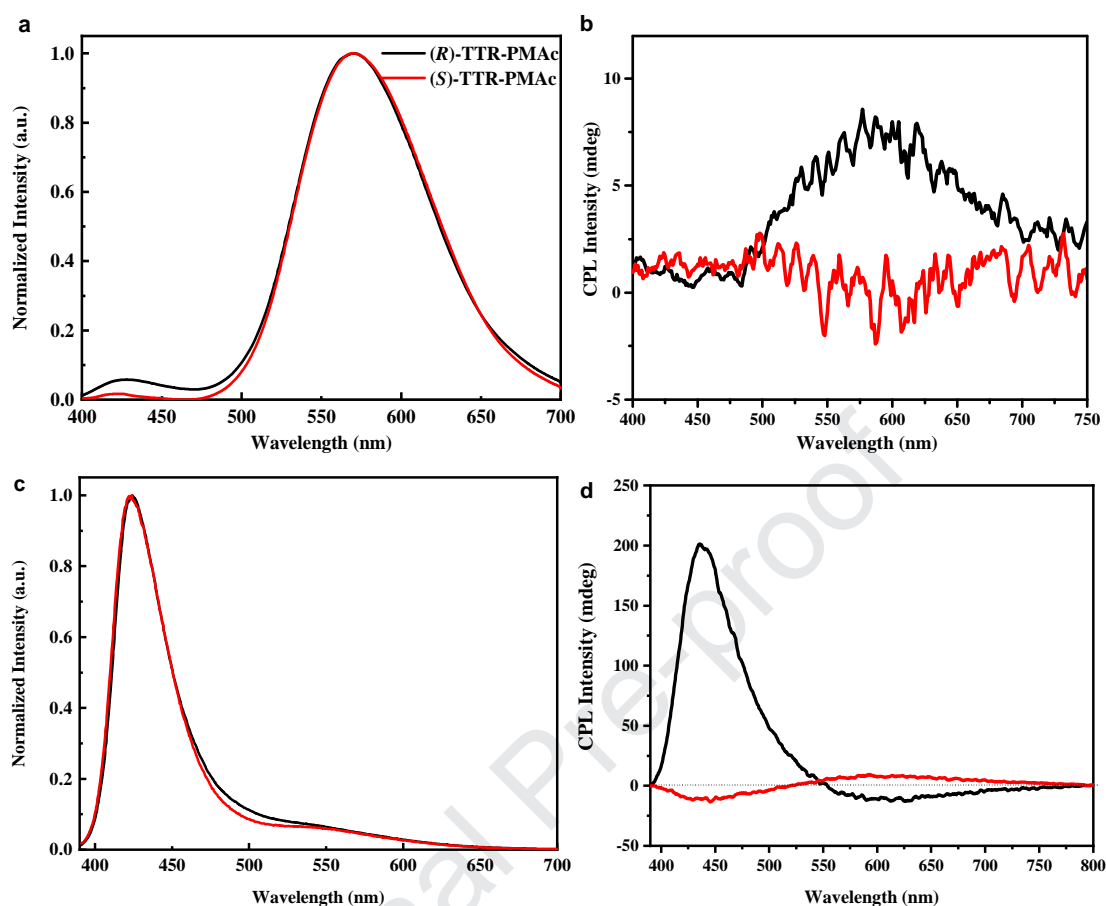


Fig.3 Emission spectra and the corresponding CPL spectra of the spin-coated pristine films derived from dilute THF solutions (a and b) (Excited at 360 nm) and powder (c and d) (Excited at 370 nm) for (*R*)- (black) and (*S*)- (red) TTR-PMAC.

4. Conclusions

In summary, we have developed a pair of chiral D moieties (*R*)- and (*S*)-PMAC, which is potentially useful for general TADF molecular design, and further constructing D-A typed TADF enantiomers (*R*)- and (*S*)-TTR-PMAC with dual stable conformations. Theoretical calculations and non-polarized measurements demonstrate their twin properties for both conformations. While under chiroptical environments, they exhibit obvious mirror-like CD and CPL properties. Thus, (*R*)- and (*S*)-PMAC are

confirmed as ideal candidates to construct CPL-TADF emitters. Moreover, by further comparing the CPL properties originated from each conformer, different properties can be clearly noticed. These results demonstrate molecular conformations can significantly influence chiroptical properties of D-A molecules and thus it is important to consider and control molecular conformations when developing such kinds of molecules.

Acknowledgments

This work was supported by the National Key Research & Development Program of China (grant number 2016YFB0401002), the National Natural Science Foundation of China (grant numbers 51533005, 51821002, 51773029), the China Postdoctoral Science Foundation (grant No. 2018M642307, 2019M661924), the Jiangsu Planned Projects for Postdoctoral Research Funds (grant number 1601241C), Collaborative Innovation Center of Suzhou Nano Science & Technology, the Priority Academic Program Development of Jiangsu Higher Education Institutions (PAPD), the 111 Project, Joint International Research Laboratory of Carbon-Based Functional Materials and Devices.

References

- [1] Sherson JF, Krauter H, Olsson RK, Julsgaard B, Hammerer K, Cirac I, et al. Quantum teleportation between light and matter. *Nature* 2006;443(7111):557-60.
- [2] Harada T, Hayakawa H, Watanabe M, Takamoto M. A solid-state dedicated circularly polarized luminescence spectrophotometer: development and application. *Appl Phys Lett* 2016;87(7):075102-5.
- [3] Kumar J, Nakashima T, Kawai T. Circularly polarized luminescence in chiral

- molecules and supramolecular assemblies. *J Phys Chem Lett* 2015;6(17):3445-52.
- [4] Shao H, He Y, Li W, Ma H. Polarization-degree imaging contrast in turbid media: a quantitative study. *Appl Opt* 2006;45(18):4491-6.
- [5] Yu N, Aieta F, Genevet P, Kats MA, Gaburro Z, Capasso F. A broadband, background-free quarter-wave plate based on plasmonic metasurfaces. *Nano Lett* 2012;12(12):6328-33.
- [6] Uoyama H, Goushi K, Shizu K, Nomura H, Adachi C. Highly efficient organic light-emitting diodes from delayed fluorescence. *Nature* 2012;492(7428):234-8.
- [7] Mehes G, Nomura H, Zhang Q, Nakagawa T, Adachi C. Enhanced electroluminescence efficiency in a spiro-acridine derivative through thermally activated delayed fluorescence. *Angew Chem Int Ed* 2012;51(45):11311-5.
- [8] Nakagawa T, Ku SY, Wong KT, Adachi C. Electroluminescence based on thermally activated delayed fluorescence generated by a spirobifluorene donor-acceptor structure. *Chem Commun* 2012;48(77):9580-2.
- [9] Zhang Q, Xiang S, Huang Z, Sun S, Ye S, Lv X, et al. Molecular engineering of pyrimidine-containing thermally activated delayed fluorescence emitters for highly efficient deep-blue ($CIE_y < 0.06$) organic light-emitting diodes. *Dyes Pigments* 2018;155:51-8.
- [10] Yuan W, Zhang M, Zhang X, Cao X, Sun N, Wan S, et al. The electron inductive effect of CF_3 on penta-carbazole containing blue emitters: trade-off between color purity and luminescent efficiency in TADF OLEDs. *Dyes Pigments* 2018;159:151-7.

- [11] Yoo SG, Song W, Lee JY. Molecular engineering of donor moiety of donor–acceptor structure for management of photophysical properties and device performances. *Dyes Pigments* 2016;128:201-8.
- [12] Li M, Li SH, Zhang D, Cai M, Duan L, Fung MK, et al. Stable enantiomers displaying thermally activated delayed fluorescence: efficient oleds with circularly polarized electroluminescence. *Angew Chem Int Ed* 2018;57(11):2889-93.
- [13] Imagawa T, Hirata S, Totani K, Watanabe T, Vacha M. Thermally activated delayed fluorescence with circularly polarized luminescence characteristics. *Chem Commun* 2015;51(68):13268-71.
- [14] Sharma N, Spuling E, Mattern Cornelia M, Li W, Fuhr O, Tsuchiya Y, et al. Turn on of sky-blue thermally activated delayed fluorescence and circularly polarized luminescence (CPL) via increased torsion by a bulky carbazolophane donor. *Chem Sci* 2019;10(27):6689-96.
- [15] Feuillastre S, Pauton M, Gao L, Desmarchelier A, Riives AJ, Prim D, et al. Design and synthesis of new circularly polarized thermally activated delayed fluorescence emitters. *J Am Chem Soc* 2016;138(12):3990-3.
- [16] Zhang MY, Li ZY, Lu B, Wang Y, Ma YD, Zhao CH. Solid-state emissive triarylborane-based [2.2]paracyclophanes displaying circularly polarized luminescence and thermally activated delayed fluorescence. *Org Lett* 2018;20(21):6868-71.
- [17] Song FY, Xu Z, Zhang QS, Zhao Z, Zhang HK, Zhao WJ, et al. Highly efficient

circularly polarized electroluminescence from aggregation-induced emission luminogens with amplified chirality and delayed fluorescence. *Adv Funct Mater* 2018;28(17):1800051-62.

[18] Xie G, Li X, Chen D, Wang Z, Cai X, Chen D, et al. Evaporation- and solution-process-feasible highly efficient thianthrene-9,9',10,10'-tetraoxide-based thermally activated delayed fluorescence emitters with reduced efficiency roll-off. *Adv Mater* 2016;28(1):181-7.

[19] Numata M, Yasuda T, Adachi C. High efficiency pure blue thermally activated delayed fluorescence molecules having 10H-phenoxaborin and acridan units. *Chem Commun* 2015;51(46):9443-6.

[20] Tsai WL, Huang MH, Lee WK, Hsu YJ, Pan KC, Huang YH, et al. A versatile thermally activated delayed fluorescence emitter for both highly efficient doped and non-doped organic light emitting devices. *Chem Commun* 2015;51(71):13662-5.

[21] Zhang Q, Li B, Huang S, Nomura H, Tanaka H, Adachi C. Efficient blue organic light-emitting diodes employing thermally activated delayed fluorescence. *Nature Photonics* 2014;8(4):326-32.

[22] Zhang Y, Zhang D, Cai M, Li Y, Zhang D, Qiu Y, et al. Towards highly efficient red thermally activated delayed fluorescence materials by the control of intra-molecular pi-pi stacking interactions. *Nanotechnology* 2016;27(9):094001.

[23] Liu XK, Chen Z, Zheng CJ, Chen M, Liu W, Zhang XH, et al. Nearly 100% triplet harvesting in conventional fluorescent dopant-based organic light-emitting

- devices through energy transfer from exciplex. *Adv Mater* 2015;27(12):2025-30.
- [24] Liu XK, Chen Z, Zheng CJ, Liu CL, Lee CS, Li F, et al. Prediction and design of efficient exciplex emitters for high-efficiency, thermally activated delayed-fluorescence organic light-emitting diodes. *Adv Mater* 2015;27(14):2378-83.
- [25] Chen JX, Wang K, Zheng CJ, Zhang M, Shi YZ, Tao SL, et al. Red organic light-emitting diode with external quantum efficiency beyond 20% based on a novel thermally activated delayed fluorescence emitter. *Adv Sci* 2018;5(9):1800436.
- [26] Shi YZ, Wang K, Li X, Dai GL, Liu W, Ke K, et al. Intermolecular charge-transfer transition emitter showing thermally activated delayed fluorescence for efficient non-doped OLEDs. *Angew Chem Int Ed* 2018;57(30):9480-4.
- [27] Wang K, Shi YZ, Zheng CJ, Liu W, Liang K, Li X, et al. Control of dual conformations: developing thermally activated delayed fluorescence emitters for highly efficient single-emitter white organic light-emitting diodes. *ACS Appl Mater Interfaces* 2018;10(37):31515-25.
- [28] Wang K, Zheng CJ, Liu W, Liang K, Shi YZ, Tao SL, et al. Avoiding energy loss on TADF emitters: controlling the dual conformations of D-A structure molecules based on the pseudoplanar segments. *Adv Mater* 2017;29(47):1701476-84.
- [29] Li W, Cai X, Li B, Gan L, He Y, Liu K, et al. Novel adamantane-substituted acridine donor for blue dual fluorescence and efficient organic light-emitting diodes. *Angew Chem Int Ed* 2018;58(2):582-6.
- [30] Tanaka H, Shizu K, Nakanotani H, Adachi C. Dual intramolecular

charge-transfer fluorescence derived from a phenothiazine-triphenyltriazine derivative.

J Phys Chem C 2014;118(29):15985-94.

[31] Zhang Z, Gao Y, Liu H, Bai Q, Li J, Liu L, et al. Dual fluorescence polymorphs: wide-range emission from blue to red regulated by TICT and their dynamic electron state behavior under external pressure. Dyes Pigments 2017;145:294-300.

[32] Wang Y, Zhang Y, Hu W, Quan Y, Li Y, Cheng Y. Circularly polarized electroluminescence of thermally activated delayed fluorescence-active chiral binaphthyl-based luminogens. ACS Appl Mater Interfaces 2019;11(29):26165-73.

[33] Song F, Xu Z, Zhang Q, Zhao Z, Zhang H, Zhao W, et al. Highly efficient circularly polarized electroluminescence from aggregation-induced emission luminogens with amplified chirality and delayed fluorescence. Adv Funct Mater 2018;28(17):1800051-62.

[34] Han JM, Guo S, Lu H, Liu SJ, Zhao Q, Huang W. Recent progress on circularly polarized luminescent materials for organic optoelectronic devices. Adv Opt Mater 2018;6(17):1800538-69.

[35] Sharma N, Spuling E, Mattern CM, Li W, Fuhr O, Tsuchiya Y, et al. Turn on of sky-blue thermally activated delayed fluorescence and circularly polarized luminescence (CPL) via increased torsion by a bulky carbazolophane donor. Chem Sci 2019;10(27):6689-96.

[36] Wu ZG, Han HB, Yan ZP, Luo XF, Wang Y, Zheng YX, et al. Chiral octahydro-binaphthol compound-based thermally activated delayed fluorescence

materials for circularly polarized electroluminescence with superior EQE of 32.6% and extremely low efficiency roll-off. *Adv Mater* 2019;31(28):1900524.

[37] Boese AD, Martin JM. Development of density functionals for thermochemical kinetics. *J Chem Phys* 2004;121(8):3405-16.

[38] Runge E, Gross EKV. Density-functional theory for time-dependent systems. *Phys Rev Lett* 1984;52(12):997-1000.

[39] Lu T, Chen F. Multiwfn: a multifunctional wavefunction analyzer. *J Comput Chem* 2012;33(5):580-92.

[40] Zhang Q, Kuwabara H, Potscavage WJ, Jr., Huang S, Hatae Y, Shibata T, et al. Anthraquinone-based intramolecular charge-transfer compounds: computational molecular design, thermally activated delayed fluorescence, and highly efficient red electroluminescence. *J Am Chem Soc* 2014;136(52):18070-81.

[41] Sun ZB, Liu JK, Yuan DF, Zhao ZH, Zhu XZ, Liu DH, et al. 2,2'-diamino-6,6'-diboryl-1,1'-binaphthyl: a versatile building block for temperature-dependent dual fluorescence and switchable circularly polarized luminescence. *Angew Chem Int Ed* 2019;58(15):4840-6.

Highlights

- Chiral donors (*R/S*)-PMAc with asymmetric carbons are for TADF molecular design.
- Enantiomers (*R/S*)-TTR-PMAc with dual conformations are designed and synthesized.
- (*R/S*)-TTR-PMAc show TADF and CPL properties.
- Chiroptical properties can be significantly influenced by molecular conformations.

Journal Pre-proof

Declaration of interests

The authors declare that they have no known competing financial interests or personal relationships that could have appeared to influence the work reported in this paper.

The authors declare the following financial interests/personal relationships which may be considered as potential competing interests: